Transcriptome and proteome analysis of nitrogen starvation responses in *Synechocystis* 6803  $\Delta glgC$ , a mutant incapable of glycogen storage

2 3 4

5

1

Damian Carrieri<sup>1+</sup>, Thomas Lombardi<sup>2</sup>, Troy Paddock<sup>1+</sup>, Melissa Cano<sup>1</sup>, Gabriel A. Goodney<sup>2</sup>, Ambarish Nag<sup>3</sup>, William Old<sup>4</sup>, Pin-Ching Maness<sup>1</sup>, Michael Seibert<sup>1</sup>, Maria Ghirardi<sup>1</sup>, and Jianping Yu<sup>1\*</sup>

6 7 8

9

10

11 12

- 1. National Renewable Energy Laboratory, Biosciences Center
- 2. Washington and Jefferson College, Computing and Information Studies
- 3. National Renewable Energy Laboratory, Computational Science Center
- 4. University of Colorado, Boulder, Department of Molecular, Cellular and Developmental Biology
- +. Current Address: Matrix Genetics, LLC.

13 14

\*corresponding author: Jianping.Yu@nrel.gov

15 16 17

18

19

20

21

22

23

24

25

26

27

28

29

30

31

32

33

34

35

36

37

#### **Abstract:**

Molecular mechanisms that regulate carbon flux are poorly understood in algae. The  $\Delta g l g C$ mutant of the cyanobacterium Synechocystis sp. PCC 6803 is incapable of glycogen storage and displays an array of physiological responses under nitrogen starvation that are different from wild-type (WT). These include non-bleaching phenotype and the redirection of photosynthetically fixed carbon towards excreted organic acids (overflow metabolism) without biomass growth. To understand the role of gene/protein expression in these responses, we followed the time course of transcripts by genome-scale microarrays and proteins by shotgun proteomics in  $\Delta g l g C$  and WT cells upon nitrogen starvation. Compared to WT, the degradation of phycobilisome rod proteins was delayed and attenuated in the mutant, and the core proteins were less degraded; both contributed to the non-bleaching appearance despite the induction of nblA genes, suggesting the presence of a break in regulation of the phycobilisome degradation pathway downstream of nblA induction. The mutant displayed NtcA-mediated transcriptional response to nitrogen starvation, indicating that it is able to sense nitrogen status. Furthermore, some responses to nitrogen starvation appear to be stronger in the mutant, as shown by the increases in transcripts for the transcriptional regulator, rre37, which regulates central carbon metabolism. Accordingly, multiple proteins involved in photosynthesis, central carbon metabolism, and carbon storage and utilization showed lower abundance in the mutant. These results indicate that the transition in the central carbon metabolism from growth to overflow metabolism in  $\Delta g l g C$ does not require increases in expression of the overflow pathway enzymes; the transition and non-bleaching phenotype are likely regulated instead at the metabolite level.

38 39 40

41

42

43

44

45

46

#### **Introduction:**

Cyanobacteria are oxygenic photosynthetic prokaryotes with potential to convert water and carbon dioxide to fuels and chemicals [1,2]. While genetic engineering offers powerful tools for working towards this goal, our fundamental understanding of complex physiological responses that result from genetic changes is incomplete. Little is known about the molecular mechanisms that regulate carbon flux in cyanobacteria, and this knowledge gap is critical in realizing the potential of algal photosynthesis.

A major topic of interest in cyanobacterial biotechnology is how to divert fixed carbon from cellular biomass to products. A common strategy is to divert metabolism from production of stored carbon reserves such as glycogen and polyhydroxyalkanoates to industrially useful compounds that are made natively or through heterologous expression of enzymes that introduce one or more foreign pathways. Towards this goal, a number of mutants incapable of storing photosynthate in these major carbon "sinks" have been generated, including those with a deletion of *glgC* encoding a glucose-1-phosphate adenylyltransferase, which is incapable of glycogen storage [3–6]. In *Synechocystis* sp. PCC 6803 (hereafter, *Synechocystis*), the *glgC* mutant grows photoautotrophically in continuous light with no decrease in growth rate, but has vastly different physiological responses to a variety of other culturing conditions such as mixotrophic growth, light/dark cycling, higher light intensities, and nitrogen deprivation than wild type (WT) [4,6].

Under nitrogen deprivation specifically, this mutant has an apparently impaired ability to degrade its phycobilisomes (photosynthetic antennae) resulting in a "non-bleaching" phenotype, whereby the cells retain a blue-green color rather than an expected yellowing resulting from phycobilisome degradation. WT cells of *Synechocystis* have a complex transcriptional response associated with nitrogen limitation, which has been well described [7]. Proteomic differences in WT cells in response to nitrogen starvation have also been thoroughly studied [8,9]. While transcription of genes encoding phycobilisome synthesis, carbon fixation, and *de novo* protein synthesis is suppressed, peptide abundances and photosynthetic activity of both Photosystems I and II are well retained within 12 hours of nitrogen removal. After 24 hours of nitrogen removal, however, nitrogen starved WT cultures lose approximately 50% of their photosynthetic activity as measured by whole cell oxygen evolution [6,7], probably due to protein damage rather than degradation [8].

Nitrogen starved cultures of *Synechocystis*  $\Delta glgC$  do not increase in biomass (as measured per dry weight or per optical density) but do convert  $CO_2$  photo-catalytically to the extracellular organic acids, alpha-ketoglutarate and pyruvate, and appear to lose photosynthetic activities at rates similar to WT while retaining phycobilisomes [6]. These responses are relevant not only to biotechnological applications, but may offer insights into the regulation of cyanobacterial physiology. It was recently proposed that the non-bleaching phenotype and other morphological phenotypes in a glycogen-deficient strain of *Synechococcus* 7002 indicated that the strain is incapable of responding to nitrogen starvation, and the remaining phycobilisomes are shown to be functionally coupled to PSII [10].

As part of the effort to develop the *Synechocystis*  $\Delta glgC$  mutant into an experimental model to study the regulation of energy and carbon metabolism in cyanobacteria, and specifically to understand molecular mechanisms that govern nitrogen starvation responses including non-bleaching phenotype and overflow metabolism, we have studied nitrogen deprivation time courses of transcripts and protein levels in WT and  $\Delta glgC$  *Synechocystis* cells by genome-scale microarray and shotgun proteomics, followed by statistical analysis of the results. An initial hypothesis was that transition from culture growth to overflow metabolism may require transcriptional and translational regulation of pathway enzymes. Here we present an overview of the similarities and differences in responses of these two strains to nitrogen starvation and highlight links or gaps between transcriptional and post-transcriptional regulations and physiological observations. Our data show that the *Synechocystis*  $\Delta glgC$  mutant is capable of sensing and responding to nitrogen starvation, and

that overflow metabolism does not require increases in pathway enzymes and instead is likely regulated at the metabolite level.

## **Materials and Methods:**

## Cell culture

The Synechocystis sp. PCC  $6803\Delta glgC$  strain was constructed from the WT strain as described previously [6]. Cultures were grown at 30°C in BG11 medium (ATCC medium 616) supplemented with 3 µM NiCl<sub>2</sub>, 20mM TES, and 100 mM NaHCO<sub>3</sub> under continuous illumination from cool white fluorescent tubes (~50 µE m<sup>-1</sup>s<sup>-1</sup>) in an atmosphere of 5% CO<sub>2</sub> in air. The antibiotic gentamicin was used at a concentration of 50 µg/mL in liquid seed cultures for inoculation from plates. Thereafter, the antibiotics were removed for growth of working cultures in BG11. For nitrogen starvation, the nitrogen source (NaNO<sub>3</sub>) in BG11 was replaced with NaCl (mol:mol) with all other components kept the same (BG11-N medium). Cells from log-phase cultures in replete medium (OD730, 0.6-0.8; dry weight, 0.3-0.5 g/L; 100 ml culture in 250 ml flasks) were harvested by centrifugation, washed, resuspended in BG11-N, and placed under the same light and atmosphere conditions as above. Optical densities were measured at 730 nm (WPA Biowave II, Biochrom). To monitor bleaching, absorbance of whole-cell suspensions of cultures were measured in a wavelength range of 300-800 nm for each time point with a spectrophotometer (DU800, Beckman Coulter). The cultures before resuspension and after resuspension in nitrate-free medium were also sampled at various time points; and 1-2 mL were centrifuged at 13,000 x g for 1 minute, the supernatants decanted, and the remaining cell pellet was cold-quenched in a dry ice / acetone bath before placing in an -80 °C freezer for later processing.

#### Extracellular metabolite determination

Cell suspensions were collected and centrifuged, and 500  $\mu$ L of the resulting cell-free supernatant was collected and combined with 100  $\mu$ L of  $D_2O$  (Sigma-Aldrich), containing 30  $\mu$ g/mL TSP (3-(trimethylsilyl)propionic-2,2,3,3-D<sub>4</sub> acid sodium salt) in a Pyrex NMR tube. Proton NMR spectra were collected with a 500-MHz, Bruker Avance-II spectrometer at 25°C; 256 scans were used with a relaxation delay of 1s using a water-suppression mode [11]. All spectra were processed using MestReNova software v 6.0.4 (Mestrelab Research S.L., Santiago de Compostela, Spain). HPLC was also used to verify identities of the metabolites in cell-free medium by comparison of retention times of the peaks relative to standards prepared in BG11-N.

#### RNA transcript and protein expression determination

For transcripts, cell pellets collected from cultures before re-suspension (t=0) and 2, 5, and 10 hours after nitrogen removal were sent to MOGENE USA (St. Louis, MO, USA) for RNA extraction and relative transcript abundance analysis by microarray (Agilent custom *Synechocystis* 6803 8-pack arrays design #017371).

For proteins, cell pellets collected from cultures before re-suspension (t=0) and 6, 12, and 24 hours after nitrogen removal were used for protein determination by shotgun proteomics. Cell pellets were thawed on ice and suspended in 1 mL deionized water. The cells were then sonicated with Misonix Sonicator 3000 equipped with a microtip for 1 minute, and the resulting suspension was used as a crude protein extract. This extract was

dried under vacuum for 2-4 hours and resuspended in 100 μL ammonium bicarbonate. The protein in ammonium bicarbonate was then reduced with 4 mM DTT at 60 °C for 10 minutes followed by alkylation with iodoacetamide (final concentration 14 mM) in darkness at room temperature (22° C) for 30 minutes. Finally a 1:50 trypsin (Sigma-Aldrich) to protein ratio was used to digest the samples at 37 °C for 24 hours. Digestion was halted with addition of formic acid at a final concentration of <1% (w:v) and then desalted by passing the working solution through PepClean C18 spin columns (Pierce) with 1,000 x g centrifugation.

Peptide samples were separated on a 2D nanoAcquity system (Waters) in 2D mode, in which peptides are fractionated into four fractions that are each then loaded and separated by an analytical column directly coupled to a Velos Orbitrap mass spectrometer. Separation was performed in the 1st dimension with a XBridge C18 NanoEase column (3 μm, 300 μm x 50 mm), equilibrated with 20 mM ammonium formate at pH 10, followed by elution in 4 steps with increasing acetonitrile concentration (2 µL/min). Each 1st dimension eluate was loaded onto the 2nd dimension column after dilution 1:9 with 0.1% (v/v) formic acid in water (20 μL/min). The analytical separation (2nd dimension) was performed on a Symmetry C18 trap column (5 µm, 180 µm x 20 mm) and a BEH130 C18 analytical column (1.7 µm, 75µm x 250 mm), equilibrated in 0.1% formic acid in water and eluted with 0.1% formic acid, 80% acetonitrile. Mass spectrometry analysis was performed using an LTO Orbitrap Velos (ThermoFisher). Survey scans were collected in the Orbitrap at 60,000 resolution (at m/z=300), and MS/MS sequencing was performed by CID in the LTQ in data-dependent mode, using monoisotopic precursor selection and rejecting singly charged and unassigned precursors for sequencing. The 10 most intense ions were targeted. After two observations of a peptide, dynamic exclusion of  $\pm 10$  ppm mass lasting 180s was applied. The maximum injection time for MS survey scans was 500 ms with 1 microscan and AGC =  $1 \times 106$ . For LTQ MS/MS scans, maximum injection time for survey scans was 250 ms with 1 microscan and AGC =  $1 \times 104$ . Peptides were fragmented by CID for 30 ms in 1 mTorr of N2 with a normalized collision energy of 35% and activation q = 0.25.

The MS/MS spectra were extracted and searched against a *Synechocystis* protein database (downloaded from UniProt in October of 2012) using the MASCOT search engine, version 2.2 (Matrix Science), with a mass tolerance on precursor ions of 25 ppm and 0.5 Da for fragment ions. The following variable modifications were considered: carbamidomethyl-Cys, methionine oxidation and pyro-glutamic acid for N-terminal Gln. Peptide identifications were accepted at a 1% FDR threshold based on a reversed protein database search. Protein assembly and label-free quantification by spectral counting was performed using Isoform Resolver [12], and protein abundance differences between FDX pull downs and controls were evaluated using a G-test [13].

#### Statistical analysis

The transcript and protein data were analyzed with R statistical computing software [14]. For the analysis of differential expression, we employed a log-likelihood ratio test [15] to compare the goodness-of-fit of two nested linear regression models of our transcript data. This approach compares the reduced linear model of the WT data (null hypothesis) to the full model comprising WT and  $\Delta glgC$  measurements (alternative hypothesis). The transcript analysis model used the geometric mean of the  $log_2(ratio)$  of the probes for each replicate, time and locus ID for WT and  $\Delta glgC$  data. If the fit of the full model including WT and  $\Delta glgC$  data is significantly better (p-value < 0.05) than that of the reduced model, then we

rejected the null hypothesis and recognized the genes as differentially expressed. We followed Mar and Quackenbush's implementation [16] with modifications to the model appropriate for our data, such as using linear regression instead of polynomial regression. We used the log-likelihood ratio test in the lmtest package in R for model comparison [17]. Since *Synechocystis* has more than 3000 genes, we adjusted our resulting p-values for multiple tests by controlling for the false discovery rate [18]. We also used the interquartile range to filter genes with low variability across all samples as these genes are unlikely to show significant differential expression [19]. The protein data were analyzed using the same process outlined above, but applied to the raw counts for each replicate and time rather than ratios. Cartesian plot and heatmap visualizations of differentially expressed proteins and gene transcripts, respectively, were created with the ggplot2 [20], gplots [21], and RColorBrewer [22] packages in R.

#### **Results and Discussion**

As observed previously [4,6,23], removal of nitrogen availability from cell cultures resulted in dramatically different physiological responses between *Synechocystis* WT and  $\Delta glgC$  strains. In the case of WT, cultures continued to increase in optical density, changed color from blue-green to yellow-green (Supplemental Figure S1), and intracellular glycogen content increased from  $7 \pm 3\%$  to  $28 \pm 3\%$  after 24 hours in nitrate-free medium (glycogen data not shown). Conversely,  $\Delta glgC$  did not increase in optical density, remained unbleached, and produced no detectable glycogen, but produced organic acids, mostly alphaketoglutarate and pyruvate, which were found extracellularly (Supplemental Figure S1).

We processed our microarray data, matched to each gene, from samples collected at 0, 2, 5, and 10 hours in biological triplicate for both WT and  $\Delta glgC$  cells as the  $\log_2(\text{ratio})$  of transcript signal between time before nitrogen removal (t=0) and 2, 5, and 10 hours after nitrogen removal for each transcript. Each time point for WT and  $\Delta glgC$  had collections for three independently treated cultures, resulting in an array of 18 values for each gene locus (3 replicates at 3 time points for 2 different strains). Because transcriptional and protein abundance responses of WT *Synechocystis* in response to nitrogen removal has been well described [7–9], we focused on the differences of these transcripts and proteins *between strains* with respect to nitrogen starvation. A list of genes with interquartile range (IQR) >1 for transcripts and the  $\log_2(\text{ratios})$  with respect to time after nitrogen removal is shown in Supplemental Table S1. The ratios of the whole transcriptome for both strains are shown in Supplemental Table S2. The comparison of all transcripts between the strains at t=0 (nitrogen replete) is shown in Supplemental Table S4, and the peptide counts from individual samples are shown in Supplemental Table S5.

Some genes are differentially expressed in nitrogen replete conditions

We first aimed to identify which genes had transcript abundances that were different between the strains during nitrogen-replete growth. Our data set includes analysis of transcripts from 3,482 genes. We calculated the geometric means of the  $\log_2(\text{ratio})$  from biological replicates comparing the WT and  $\Delta g l g C$  strains. Despite identical growth rates

under our growth conditions (leading up to time 0 hours), 23 genes had transcript abundances with a log<sub>2</sub>(ratio) of a magnitude larger than 1.5 (Table 1).

Among the genes whose transcripts are expressed at levels higher in the  $\Delta glgC$  mutant than WT are the glutamine synthetase inactivation factors IF7 and IF17 (ssl1911 and sll1515, respectively). These genes are known to be up-regulated under oxidative stress induced by addition of hydrogen peroxide [24]. Interestingly,  $\Delta glgC$  was reported to have a high light sensitivity and severely restricted viability on agar plates containing glucose [4].

Among the genes whose transcripts are expressed at levels lower in  $\Delta glgC$  than WT, are sll1688 encoding threonine synthase and slr0884 encoding glyceraldehyde 3-phosphate dehydrogenase. The largest difference by far was for that of the glgC gene. Although the theoretical ratio in transcript abundance of the glgC transcript between the mutant and WT is infinitely small, some background signal contributes to transcript abundance ratio measurements. This value is much larger in magnitude than any  $\log_2(\text{ratio})$  observed at the start of the experiment.

Table 1: Genes with transcript abundance  $log_2(ratios)$  with a magnitude greater than 1.5 ( $\Delta g lg C$  mutant versus wild-type under nitrogen-replete conditions, i.e. t=0)

Locus	<u>Annotation</u>	<u>Ratio</u> <sup>a</sup>	<u>Log₂(Ratio)</u>	
slr1634	hypothetical protein	8.16	3.03	
sll5036	sulfide-quinone reductase	3.75	1.91	
slr5037	hypothetical protein	3.50	1.81	
ssl1911	glutamine synthetase inactivating factor IF7	3.49	1.80	
sll1515	glutamine synthetase inactivating factor IF17	3.21	1.68	
sll0720	RTX toxin activating protein homolog	3.03	1.60	
sll1688	threonine synthase	0.34	-1.56	
slr1287	hypothetical protein	0.34	-1.58	
slr0334	unknown protein	0.34	-1.58	
slr7092	hypothetical protein	0.33	-1.58	
slr0749	light-independent protochlorophyllide reductase iron protein subunit ChIL	0.33	-1.59	
sll1723	probable glycosyltransferase	0.33	-1.59	
slr0884	glyceraldehyde 3-phosphate dehydrogenase 1 (D+)	0.32	-1.66	
sll7090	unknown protein	0.31	-1.67	
slr0096	Low Affinity sulfate transporter	0.31	-1.68	
sll0474	two-component hybrid sensor and regulator	0.31	-1.71	
ssr1251	hypothetical protein	0.29	-1.78	
slr6108	hypothetical protein	0.28	-1.84	
slr6072	unknown protein	0.27	-1.87	
sll1483	periplasmic protein, similar to transforming growth factor induced protein	0.24	-2.04	
ssr7093	hypothetical protein	0.21	-2.23	
slr0199	hypothetical protein	0.14	-2.83	
slr1176	glucose-1-phosphate adenylyltransferase	0.02	-5.50	

a. Ratio of the transcript abundance of the  $\Delta glgC$  mutant / wild-type.

Various amino acid synthesis pathways show differential expression in nitrogen starvation

We next sought to identify genes in the two strains that had significantly different transcript abundance profiles with respect to time after nitrogen removal. To do this, we performed a log-likelihood ratio test (LRT) on our microarray dataset using the log<sub>2</sub>(ratios) of transcript abundances at times 2, 5, and 10 hours after nitrogen removal relative to t=0 (nitrogen replete conditions) and used independent culture replicate data for each time point. The LRT computational approach was chosen because of its strong statistical power and

specific applicability to large datasets that change dynamically over time [25]. We chose an adjusted p-value of <0.05 as our threshold to identify genes with transcripts that had significantly different abundance ratio changes over time. We also set a threshold for the interquartile range (IQR) to >1 to filter for genes with larger changes in transcript ratios. From this analysis, 228 genes were identified (Supplemental Table S1). To highlight the genes with the largest magnitude change differences (interquartile range values) in transcript over time, we list the top 10 genes and their relevant values in Figure 1.

We note that the top listed gene, thrC (sll1688) encoding threonine synthase, has a lower transcript level in nitrogen replete conditions and shows dramatic down regulation in WT relative to  $\Delta glgC$  in response to nitrogen removal, while relatively constant expression of thrC is observed in  $\Delta glgC$  cells. This is an indication that threonine synthase protein abundances may be higher in  $\Delta glgC$  than in WT. Indeed, threonine synthase peptides showed much higher levels at all times in  $\Delta glgC$  compared to WT by our proteomic analysis (Figure 2).

As with transcripts, we aimed to investigate the differences in protein abundances between  $\Delta glgC$  and WT cells. We executed a likelihood ratio test with our proteomic data, much like our analysis of the microarray data, but using raw peptide abundance values rather than  $log_2(values)$  for input. Of 1,050 proteins detected, 74 proteins had peptide abundance profiles that were significantly different with a threshold of p < 0.05 (See Supplemental Table S4 for a full list).

Other proteins involved in amino acid metabolism, including 2-isopropylmalate synthase, glycine dehydrogenase, gamma-glutamyl phosphate reductase, and the amidotransferase HisH were found to have significantly different peptide abundance profiles. Their relative abundances are shown along with those of threonine synthase in Figure 2. While threonine synthase and 2-isopropylmalate synthase (LeuA) are higher in abundance in  $\Delta glgC$  than WT cells, the other proteins mentioned have the opposite relationship. The enzyme 2-isopropylmalate synthase (LeuA) is involved in leucine synthesis from acetyl-CoA and as an intermediate yielding  $\alpha$ -keto-isocaproate (KIC). We detected very small quantities of KIC in the extracellular medium of nitrogen starved *Synechocystis*  $\Delta glgC$  cultures, but not in abundances that we considered noteworthy. However, this is a dominant overflow metabolite in nitrogen starved cultures of  $\Delta glgC$  in *Synechococcus* sp. PCC 7002 [26].

It is important to note that relative peptide abundance counts cannot be compared between different protein subunits due to methodology, so no conclusions will be drawn here based on peptide counts between different proteins.

We also note that peptide counts for a given protein in our analysis are normalized to the total amount of equally loaded protein from each mass spectrometry run, in effect giving a peptide abundance ratio relative to total peptides detected. If this is a reasonable treatment, we would expect a constitutive set of detected proteins, such as the ribosomes, to give a relatively steady signal across the time course of nitrogen starvation. We performed this analysis and observed that the sum of the peptide counts assigned to 30S and 50S ribosomal subunits do not change substantially with respect to time (See Supplemental Figure S2). The total sums of the peptide counts for non-phycobilisome proteins were also relatively constant overtime in both strains (not shown). The most abundant proteins that have changed differently between the WT and mutant cell lines in nitrogen starvation were the phycobilisomes. Normalization of the peptide counts for the 74 proteins identified by our

analysis to either the alpha or beta subunit of phycocyanin resulted in the same qualitative differences in protein abundances between WT and mutant strains (not shown).

*Transcriptional regulators Rre37 and RreP are highly induced in*  $\Delta$ *glgC* 

From Figure 1, it can be seen that transcriptional regulators rre37 (sll1330) and rreP (slr6040) have large and significantly different transcriptional changes over time in nitrogen-depleted  $\Delta glgC$  respective to WT, increasing significantly higher in the mutant.

Rre37 typically controls expression of an array of glycolytic genes [27], sugar catabolic genes [28], fructose 1,6-bisphosphate aldolase (FBA), which is involved in both glycolytic and photosynthetic reactions [29], and genes related to the tricarboxylic acid cycle and pyruvate metabolism [30]. Its transcription is regulated in part by NtcA [31], a transcription factor belonging to the cAMP receptor protein family. It is well documented that NtcA can perceive nitrogen status in cyanobacteria by sensing levels of alphaketoglutarate [32]. We found that transcript levels of ntcA (sll1423) did not change significantly in either WT or mutant cells (Supplemental Figure S3). Rre37 also stimulates accumulation of alpha-ketoglutarate [31]. Some, but not all previously shown transcripts affected by Rre37 were stimulated differentially in  $\Delta glgC$ .

RreP (slr6040) is a transcriptional regulator from the plasmid encoded hik31 operon in Synechocystis. In this model organism, there are two hik31 operons similar in sequence, one of which is encoded in the chromosome (sll0788-0790) and the other on the pSYSX plasmid (slr0639-0641) [33]. The plasmid-encoded operon was shown to be an important regulator of central carbon metabolism as well as cell division in the dark [34], and it is important in regulating the ability of Synechocystis to adapt to the presence of glucose [35] by positively affecting genes involved in heterotrophy [33]. A member of the chromosomal hik31 operon is stimulated by the presence of hydrogen peroxide [36] and is involved in negative control of autotrophic events [33]. Members of both hik31 operons were differentially expressed in  $\Delta glgC$  relative to WT in our samples (Figure 3). None of these proteins, nor Rre37, were detected in any samples by our proteomic measurements.

Central carbon metabolism enzymes are generally lower in  $\Delta glgC$  after prolonged nitrogen starvation

Given the observation of dramatically different expression patterns of *rre37* and the *hik31* operons and the fact that *glg*C is itself an important gene for carbon storage, we were interested in investigating expression levels of proteins involved in central carbon metabolism, especially the enzymes involved in glycogen, pyruvate, and AKG.

Of the 74 proteins found in our analysis to have peptide abundance profiles that were significantly different between strains (with a threshold of p < 0.05), 8 proteins can be considered to have key central carbon metabolism or carbon storage function by geneannotation. Peptides assigned to GlgC were significantly counted above the limit of detection of our protocol in WT but not the  $\Delta glg$ C samples (Supplemental table S4). Also related to glycogen metabolism, GlgA and GlgX peptides were counted roughly 2-fold lower in the mutant at 12 and 24 hours during nitrogen starvation (Figure 4). Regarding another carbon storage pathway, PhaB, an acetoacetyl-CoA reductase required for polyhydroxyalkanoate

synthesis, is expressed at a 2-fold lower level in later nitrogen starvation time points in the mutant than WT (Figure 4).

All proteins we related to central carbon metabolism identified in our analysis were expressed at lower abundances in  $\Delta g l g C$  than in WT in later stages of nitrogen starvation. These proteins include pyruvate kinase (Pyk1), acetate kinase (AckA), pyruvate flavodoxin oxidoreductase (NifJ), fructose-bisphosphate aldolase (Fda, Class I), and a subunit of succinate dehydrogenase flavoprotein (SdhA) as shown in Figure 5. Many of the genes that encode these proteins were shown to be expressed less in an *rre37* overexpression mutant than WT in *Synechocystis* after four hours of nitrogen starvation, including Pyk1, AckA, and SdhA [30]. This is consistent with our observations that peptide abundances of the above listed proteins are lower in  $\Delta g l g C$  cells, which have strong increases in transcripts of *rre37* as nitrogen starvation proceeds. In the WT, the abundance of these enzymes (Figure 5) increased in response to nitrogen starvation, whereas this response appears to be mostly or entirely missing in the  $\Delta g l g C$  cells, suggesting that  $\Delta g l g C$  may lack the regulatory processes that lead to a corresponding increase in WT levels of these enzymes.

A scheme involving many of the enzymes discussed here is provided for context in Figure 6. It is noteworthy that most of the proteins are present at lower levels in  $\Delta glgC$ .

The observation of generally lower protein abundances of the central carbon metabolism enzymes in the mutant disputes our starting hypothesis (postulated before inspection of these data) that differential protein expression is responsible for preferentially up-regulating carbon flux in pathways that lead to excreted organic acids (mostly AKG and pyruvate). Furthermore, the differences in transcripts associated with catabolism may well be a secondary result of the metabolic differences between WT and  $\Delta glgC$ . While WT cells respond metabolically to nitrogen starvation by storing energy and reductant as glycogen,  $\Delta glgC$  cells are unable to do this and thus have a different metabolic profile characterized by "overflow metabolism".

Differentially lowered expression of RuBisCO, Photosystem I, and ATP synthase genes in  $\Delta glgC$ .

Previous studies have reported continued photosynthesis of  $\Delta glgC$  under nitrogen starvation leading to accumulation of extracellular organic acids from newly fixed carbon [4,6]. From filtering our microarray data for genes with significant transcriptional responses to nitrogen starvation (Supplemental Table S1), we identified several genes involved in photosynthesis (Figure 7). We noted a severely lowered transcription of the *rbc* operon, encoding the subunits for ribulose-1,5-bispohsphate carboxylase/oxygenase (RuBisCO) in the WT after 10 hours of nitrogen removal, but even more so in  $\Delta glgC$ . Transcripts of many genes encoding subunits of photosystem I were also lower, but more so in  $\Delta glgC$ . Furthermore, the gene encoding the gamma subunit of ATP synthase (ssl2615, AtpH) had a lower transcript level in  $\Delta glgC$  than in WT (Figure 7).

However, the transcriptional changes were often not reflected in protein abundance measurements. In addition to the mismatch in threonine synthase mentioned above, see the case of RuBisCO large and small subunits (Figure 7, 8). While their transcript levels decreased significantly within 2 hours in the mutant, and decreased more slowly in the WT, peptide counts were relatively stable in both strains over 24 hours. These differences in

transcriptional responses versus actual peptide counts are clear examples of why observations of transcriptional changes alone must be interpreted with caution.

Huang *et al.* observed a similar phenomenon in WT *Synechocystis* when measuring both protein and transcript abundances in response to nitrogen starvation [8]. While all transcripts for the phycobilisome, Photosystem II, Photosystem I, cytochrome b6/f complex, photosynthetic electron transport, and F-type ATPase were down-regulated by 2 to 38 fold, 17 photosynthetic proteins had *increased* counts at the peptide levels. Their interpretation of these data was that cells stopped transcription of photosynthetic genes in order to save energy but did not degrade the proteins that were intact at the time of nitrogen removal.

Our interpretation of these data is consistent with Huang's. We suggest that dramatic down-regulation of transcripts involved in photosynthesis, ATP production, and carbon fixation reflect an unusually high carbon: nitrogen ratio in the cells, because the cells are also starved of nitrogen, *de novo* protein synthesis is compromised, and through a currently unknown mechanism, protein degradation rates observed for nutrient replete cells are severely slowed in response to a limited availability of amino acids. Further experimentation on metabolic fluxes and their effects on transcription and translation would be valuable to test this hypothesis. It is notable that RuBisCO proteins are one of the most abundant class of proteins detected in the cell, the other being phycobilisomes.

Phycobilisome degradation is unsuccessfully executed in the  $\Delta glgC$  strain despite the induction of nblA overexpression

From analysis of peptide abundances, the phycobilisome structural proteins encoding phycocyanin were among those with different abundance profiles when comparing WT and mutant. Figure 9 shows the peptide abundances of both structural subunits (alpha and beta) of two structural protein hetero-dimers in the phycobilisome, phycocyanin and allophycocyanin. The differences between WT and mutant support observations of a 'nonbleaching' phenotype in  $\Delta g l g C$  cells (Supplemental Figure S1) but suggest that the main difference between WT and  $\Delta g l g C$  phycobilisomes is a smaller, but not insignificant, loss of phycocyanin in  $\Delta g l g C$  cells. However, peptide abundances of most of the structural subunits decreased over time (the beta subunit of allophycocyanin in  $\Delta g l g C$  cells being the exception). Jackson et al. recently showed that remaining phycobilisomes in  $\Delta glgC$  cells of Synechococcus sp. PCC 7002 remain coupled to Photosystem II [10]. This could indicate that the non-bleaching phenotype underlies a difference between the mutant and WT strains in energy distribution between PSII and PSI, which would possibly be reflected in the identity and abundance of extracellular metabolites that appear in nitrogen starved  $\Delta g l g C$  cultures. Future experiments involving 77 K fluorescence measurements and metabolite characterizations could be enlightening.

The observation that  $\Delta glgC$  cells do not degrade their phycocyanin as fast as WT also suggests a major difference in amino acid recycling. Because phycobilisomes can consist of as much as 50% of cell protein under nutrient replete conditions, it is often suggested that these proteins serve as peptide reserves for cells to use under nutrient limitation for more essential functions [37]. It has been reported that glucose feeding to *Synechocystis* under nitrogen deplete conditions inhibits phycocyanin degradation [38], and we have observed this in our laboratory (data not shown). A key step in phycobilisome degradation pathway is the induction of nblA expression. We determined that both nblA1 and nblA2 transcripts are

increased in  $\Delta glg$ C during nitrogen starvation, similar to WT (Supplemental Figure S6), thus we speculate that the non-bleaching appearance is due to a difference in the phycobilisome degradation pathway downstream of nblA induction in  $\Delta glg$ C cells and is associated with the absence of glycogen synthesis. We were unable to detect NblA proteins directly by our proteomic approach, however, so further justification for this hypothesis is needed.

# *Hydrogenase subunits are induced in* $\Delta$ glgC

From analysis of proteins that have different expression profiles in the mutant versus WT, we found a strong difference in the presence of all five subunits of the bidirectional hydrogenase. The hydrogenase, encoded by the hox operon, is present in many but not all cyanobacteria. The role of this enzyme in cyanobacterial metabolism, including photosynthesis and respiration has been elusive, but some evidence supports the hypothesis that the bidirectional hydrogenase has a role as a redox regulator by some interplay via the NAD(P)(H) pools [39]. In nitrogen starved conditions, WT cyanobacteria accumulate a substantial amount of glycogen and down regulate photosynthetic activity, which is likely to affect redox ratios of NAD<sup>+</sup>/NADH and NADP<sup>+</sup>/NADPH. Indeed, a substantial increase in hydrogenase activity has been measured in nitrate-limited, aerobic cultures of cyanobacteria such as Gloeocapsa alpicola CALU 743 without an associated increases in transcript abundances [40]. We observed only minor changes (less than 2.5 fold, or a  $\log_2(\text{ratio}) < 1.4$ ) in hox hydrogenase transcript expression 10 hours after nitrogen removal in WT (not shown), yet peptide abundances of all subunits of this enzyme increased substantially after 12 hours of nitrogen removal in WT but to a lesser extent in  $\Delta glgC$  (Supplemental Figure S7). Although these peptides were present, Hox hydrogenase is not known to function under aerobic conditions.

Nitrogen status is sensed, and NtcA-mediated response is initiated by  $\Delta glgC$ 

Having assessed which transcripts and proteins were differentially expressed between WT and  $\Delta g l g C$ , it is important to note similarities between the strains regarding nitrogen status sensing. While the typical response regulators and other typical NtcA-mediated transcriptional changes as reported by Krasikov *et al.* [7] and others were observed for our WT cells, very similar responses were found in  $\Delta g l g C$ . Heat maps of transcriptional changes observed for genes associated with global nitrogen regulation, nitrogen assimilation, amino acid biosynthesis, and pigment losses (or "bleaching") are presented in Supplemental Figures S3-S6, which can be easily compared to those of Krasikov *et al.* [7]. The response patterns of genes associated with these processes are remarkably similar between our WT and glgC strains, which clearly show that nitrogen status is indeed sensed and the typical NtcA-mediated response is initiated in  $\Delta g l g C$  cells.

Conclusions

Here we have highlighted some differences and similarities in transcript and protein expression in response to nitrogen starvation in  $\Delta glgC$  and WT cells of *Synechocystis*. The non-bleaching phenotype, which has implication in energy distribution between PSII and

PSI, is attributed to delayed and attenuated degradation of phycobilisome rod and core proteins, likely due to a lesion in the phycobilisome degradation pathway downstream of the induction of nblA transcription. In the absence of glycogen synthesis, glycogen degradation genes are down-regulated. Contrary to a recent proposal [10] based on study in Synechococcus sp. PCC 7002  $\Delta glgC$ , there are clear similarities between Synechocystis  $\Delta glgC$  and WT in transcriptional responses associated with nitrogen starvation, indicating that nitrogen status is indeed sensed by the mutant. Also contrary to our initial hypothesis, there were no increases in abundance of enzymes associated with pathways leading to the excreted organic acids. Taken together, these data suggest that both non-bleaching phenotype and overflow metabolism should not be attributed to a difference between the strains in transcriptional responses associated with nitrogen status sensing. We propose that these phenotypes likely arise instead from differences in the metabolic status of the cells related to the absence of glycogen synthesis, and may involve mechanisms such as allosteric regulation of key enzymes. Future studies to further characterize metabolic changes would be enlightening.

# Acknowledgments

- Project planning, sample preparation, physiological characterization, and acquisition of
- transcriptomic and proteomic data were supported by National Renewable Energy
- Laboratory LDRD program (MS, JY, PCM, DC, TP, CC, AN). In-depth data analyses and
- preparation of the manuscript was supported by the U.S. Department of Energy (DOE),
- Office of Science Basic Energy Sciences (MG, DC, TP, MC, JY). This work was also
- supported in part by DOE Office of Energy Efficiency and Renewable Energy, Fuel Cell
- Technologies Office (PCM), and by a RASEI Seed Grant for proteome analysis (MS,
- WO). The authors wish to thank Patrick H Bradley, Shihui Yang, and Carrie Eckert for
- discussions, comments on the manuscript, and technical assistance. The U.S. Government
- retains and the publisher, by accepting the article for publication, acknowledges that the U.S.
- Government retains a nonexclusive, paid up, irrevocable, worldwide license to publish or
- reproduce the published form of this work, or allow others to do so, for U.S. Government
- 516 purposes.

517

518

503

## **Conflict of interest**

- D Carrieri and T Paddock are now employed at Matrix Genetics, LLC, a company that
- engineers cyanobacteria strains of commercial interest.

521

522

## **Author Contributions**

- 523 JY, MS, PCM and CC planned the project; DC and TP planned and performed the
- 524 physiological experiments and collected cell samples and proteins; WO performed
- 525 proteomics analysis; DC, AN, CC, TL, GAG performed statistical analyses; DC, TL, GAG,
- 526 TP, MC, PCM, MG and JY interpreted data and drafted the manuscript; all authors edited
- and approved the manuscript.

<b>500</b>	D C	
530	Reference	C

- 533 [1] S.A. Angermayr, K.J. Hellingwerf, P. Lindblad, M.J. Teixeira de, Energy 534 biotechnology with cyanobacteria, Curr. Opin. Biotechnol. 20 (2009) 257–263.
- 535 [2] D.C. Ducat, J.C. Way, P.A. Silver, Engineering cyanobacteria to generate high-value products, Trends Biotechnol. 29 (2011) 95–103.
- Y. Xu, L. Tiago Guerra, Z. Li, M. Ludwig, G. Charles Dismukes, D.A. Bryant,
   Altered carbohydrate metabolism in glycogen synthase mutants of Synechococcus sp.
   strain PCC 7002: Cell factories for soluble sugars, Metab. Eng. 16 (2013) 56–67.
- 540 [4] M. Gründel, R. Scheunemann, W. Lockau, Y. Zilliges, Impaired glycogen synthesis 541 causes metabolic overflow reactions and affects stress responses in the 542 cyanobacterium Synechocystis sp. PCC 6803, Microbiol. (United Kingdom). 158 543 (2012) 3032–3043.
- J.W. Hickman, K.M. Kotovic, C. Miller, P. Warrener, B. Kaiser, T. Jurista, et al.,
   Glycogen synthesis is a required component of the nitrogen stress response in
   Synechococcus elongatus PCC 7942, Algal Res. 2 (2013) 98–106.
- 547 [6] D. Carrieri, T. Paddock, P.-C. Maness, M. Seibert, J. Yu, Photo-catalytic conversion 548 of carbon dioxide to organic acids by a recombinant cyanobacterium incapable of 549 glycogen storage, Energy Environ. Sci. 5 (2012) 9457–9461.
- V. Krasikov, E. Aguirre von Wobeser, H.L. Dekker, J. Huisman, H.C.P. Matthijs,
   Time-series resolution of gradual nitrogen starvation and its impact on photosynthesis
   in the cyanobacterium Synechocystis PCC 6803, Physiol. Plant. 145 (2012) 426–439.
- 553 [8] S. Huang, L. Chen, R. Te, J. Qiao, J. Wang, W. Zhang, Complementary iTRAQ 554 proteomics and RNA-seq transcriptomics reveal multiple levels of regulation in 555 response to nitrogen starvation in Synechocystis sp. PCC 6803, Mol. Biosyst. 9 (2013) 556 2565–74.
- 557 [9] K.M. Wegener, A.K. Singh, J.M. Jacobs, T. Elvitigala, E. a Welsh, N. Keren, et al.,
  558 Global proteomics reveal an atypical strategy for carbon/nitrogen assimilation by a
  559 cyanobacterium under diverse environmental perturbations, Mol. Cell. Proteomics. 9
  560 (2010) 2678–2689.
- [10] S. Jackson, J.J. Eaton-Rye, D. Bryant, M.C. Posewitz, F.K. Davies, Dynamics of
   Photosynthesis in the Glycogen-Deficient glgC Mutant of Synechococcus sp. PCC
   7002, Appl. Environ. Microbiol. 81 (2015) AEM.01751–15.
- 564 [11] D. Carrieri, K. McNeely, A.C. De Roo, N. Bennette, I. Pelczer, G.C. Dismukes,

- Identification and quantification of water-soluble metabolites by cryoprobe-assisted
- nuclear magnetic resonance spectroscopy applied to microbial fermentation., Magn.
- 567 Reson. Chem. 47 Suppl 1 (2009) S138–46.
- 568 [12] K. Meyer-Arendt, W.M. Old, S. Houel, K. Renganathan, B. Eichelberger, K.A.
- Resing, et al., IsoformResolver: A peptide-centric algorithm for protein inference, J.
- 570 Proteome Res. 10 (2011) 3060–3075.
- 571 [13] W.M. Old, Comparison of Label-free Methods for Quantifying Human Proteins by
- 572 Shotgun Proteomics, Mol. Cell. Proteomics. 4 (2005) 1487–1502.
- 573 [14] R Development Core Team, R: A language and environment for statistical computing.
- R Foundation for Statistical Computing, Vienna, Austria., R Found. Stat. Comput.
- 575 Vienna, Austria. (2015).
- 576 [15] K.Y. Seng, R.W. Glenny, D.K. Madtes, M.E. Spilker, P. Vicini, S.A. Gharib,
- Comparison of statistical data models for identifying differentially expressed genes
- using a generalized likelihood ratio test, Gene Regul Syst Bio. 2 (2008) 125–139.
- 579 [16] J.C. Mar, J. Quackenbush, Decomposition of gene expression state space trajectories,
- 580 PLoS Comput. Biol. 5 (2009) e1000626.
- 581 [17] A. Zeileis, T. Hothorn, Diagnostic checking in regression relationships, R News. 2
- 582 (2002) 7–10.
- 583 [18] Y. Benjamini, Y. Hochberg, Controlling the false discovery rate: a practical and
- powerful approach to multiple testing, J. R. Stat. Soc. B. 57 (1995) 289–300.
- 585 [19] L. Torgo, Data Mining with R: Learning with Case Studies, Chapman and Hall/CRC,
- 586 2010.
- 587 [20] H. Wickham, ggplot2: Elegant Graphics for Data Analysis, Springer-Verlag, New
- 588 York, 2009.
- 589 [21] G.R. Warnes, B. Bolker, L. Bonebakker, R. Gentleman, W.H.A. Liaw, T. Lumley, et
- al., gplots: Various R Programming Tools for Plotting Data., R Packag. Version
- 591 2.17.0. (2015).
- 592 [22] E. Neuwirth, ColorBrewer Palettes, R Packag. Version. (2014).
- 593 [23] D. Carrieri, C. Broadbent, D. Carruth, T. Paddock, J. Ungerer, P.C. Maness, et al.,
- Enhancing photo-catalytic production of organic acids in the cyanobacterium
- 595 Synechocystis sp.PCC 6803 ??glgC, a strain incapable of glycogen storage, Microb.
- 596 Biotechnol. 8 (2015) 275–280.
- 597 [24] Y. Kanesaki, H. Yamamoto, K. Paithoonrangsarid, M. Shoumskaya, I. Suzuki, H.

- Hayashi, et al., Histidine kinases play important roles in the perception and signal transduction of hydrogen peroxide in the cyanobacterium, Synechocystis sp. PCC 600 6803, Plant J. 49 (2007) 313–324.
- [25] J.D. Storey, W. Xiao, J.T. Leek, R.G. Tompkins, R.W. Davis, Significance analysis of
   time course microarray experiments, Proc. Natl. Acad. Sci. U. S. A. 102 (2005)
   12837–12842.
- [26] F.K. Davies, V.H. Work, A.S. Beliaev, M.C. Posewitz, Engineering Limonene and
   Bisabolene Production in Wild Type and a Glycogen-Deficient Mutant of
   Synechococcus sp. PCC 7002, Front. Bioeng. Biotechnol. 2 (2014) 21.
- 607 [27] Y. Tabei, K. Okada, M. Tsuzuki, Sll1330 controls the expression of glycolytic genes 608 in Synechocystis sp. PCC 6803, Biochem. Biophys. Res. Commun. 355 (2007) 1045– 609 1050.
- 610 [28] M. Azuma, T. Osanai, M.Y. Hirai, K. Tanaka, A response regulator Rre37 and an RNA polymerase sigma factor SigE represent two parallel pathways to activate sugar catabolism in a cyanobacterium synechocystis sp. PCC 6803, Plant Cell Physiol. 52 (2011) 404–412.
- 614 [29] Y. Tabei, K. Okada, E. Horii, M. Mitsui, Y. Nagashima, T. Sakai, et al., Two 615 regulatory networks mediated by light and glucose involved in glycolytic gene 616 expression in cyanobacteria, Plant Cell Physiol. 53 (2012) 1720–1727.
- [30] H. Iijima, A. Watanabe, J. Takanobu, M.Y. Hirai, T. Osanai, Rre37 overexpression
   alters gene expression related to the tricarboxylic acid cycle and pyruvate metabolism
   in synechocystis sp. PCC 6803, Sci. World J. 2014 (2014).
- [31] A. Joseph, S. Aikawa, K. Sasaki, H. Teramura, T. Hasunuma, F. Matsuda, et al., Rre37
   stimulates accumulation of 2-oxoglutarate and glycogen under nitrogen starvation in
   Synechocystis sp. PCC 6803, FEBS Lett. 588 (2014) 466–471.
- [32] M.I. Muro-Pastor, J.C. Reyes, F.J. Florencio, Cyanobacteria Perceive Nitrogen Status
   by Sensing Intracellular 2-Oxoglutarate Levels, J. Biol. Chem. 276 (2001) 38320–
   38328.
- [33] S. Nagarajan, D.M. Sherman, I. Shaw, L.A. Sherman, Functions of the duplicated
   hik31 operons in central metabolism and responses to light, dark, and carbon sources
   in synechocystis sp. strain PCC 6803, J. Bacteriol. 194 (2012) 448–459.
- [34] S. Nagarajan, S. Srivastava, L.A. Sherman, Essential role of the plasmid hik31 operon
   in regulating central metabolism in the dark in Synechocystis sp. PCC 6803, Mol.
   Microbiol. 91 (2014) 79–97.

<ul><li>632</li><li>633</li><li>634</li></ul>	[35]	S. Kahlon, K. Beeri, H. Ohkawa, Y. Hihara, O. Murik, I. Suzuki, et al., A putative sensor kinase, Hik31, is involved in the response of Synechocystis sp. strain PCC 6803 to the presence of glucose, Microbiology. 152 (2006) 647–655.
635 636 637	[36]	H. Li, A.K. Singh, L.M. Mcintyre, a Louis, L. a Sherman, Differential Gene Expression in Response to Hydrogen Peroxide and the Putative PerR Regulon of Synechocystis sp. Strain PCC 6803, J. Bacteriol. 186 (2004) 3331–3345.
638 639 640	[37]	R. Schwarz, a R. Grossman, A response regulator of cyanobacteria integrates diverse environmental signals and is critical for survival under extreme conditions, Proc. Natl. Acad. Sci. U. S. A. 95 (1998) 11008–11013.
641 642 643	[38]	K. Elmorjani, M. Herdman, Metabolic Control of Phycocyanin Degradation in the Cyanobacterium Synechocystis PCC 6803: a Glucose Effect, Microbiology. 133 (1987) 1685–1694.
644 645 646	[39]	D. Carrieri, K. Wawrousek, C. Eckert, J. Yu, P.C. Maness, The role of the bidirectional hydrogenase in cyanobacteria, Bioresour. Technol. 102 (2011) 8368–8377.
647 648 649 650	[40]	M.E. Sheremetieva, O.Y. Troshina, L.T. Serebryakova, P. Lindblad, Identification of hox genes and analysis of their transcription in the unicellular cyanobacterium Gloeocapsa alpicola CALU 743 growing under nitrate-limiting conditions, FEMS Microbiol. Lett. 214 (2002) 229–233.
651		

# **Figures**

652

653

654 655

656

657



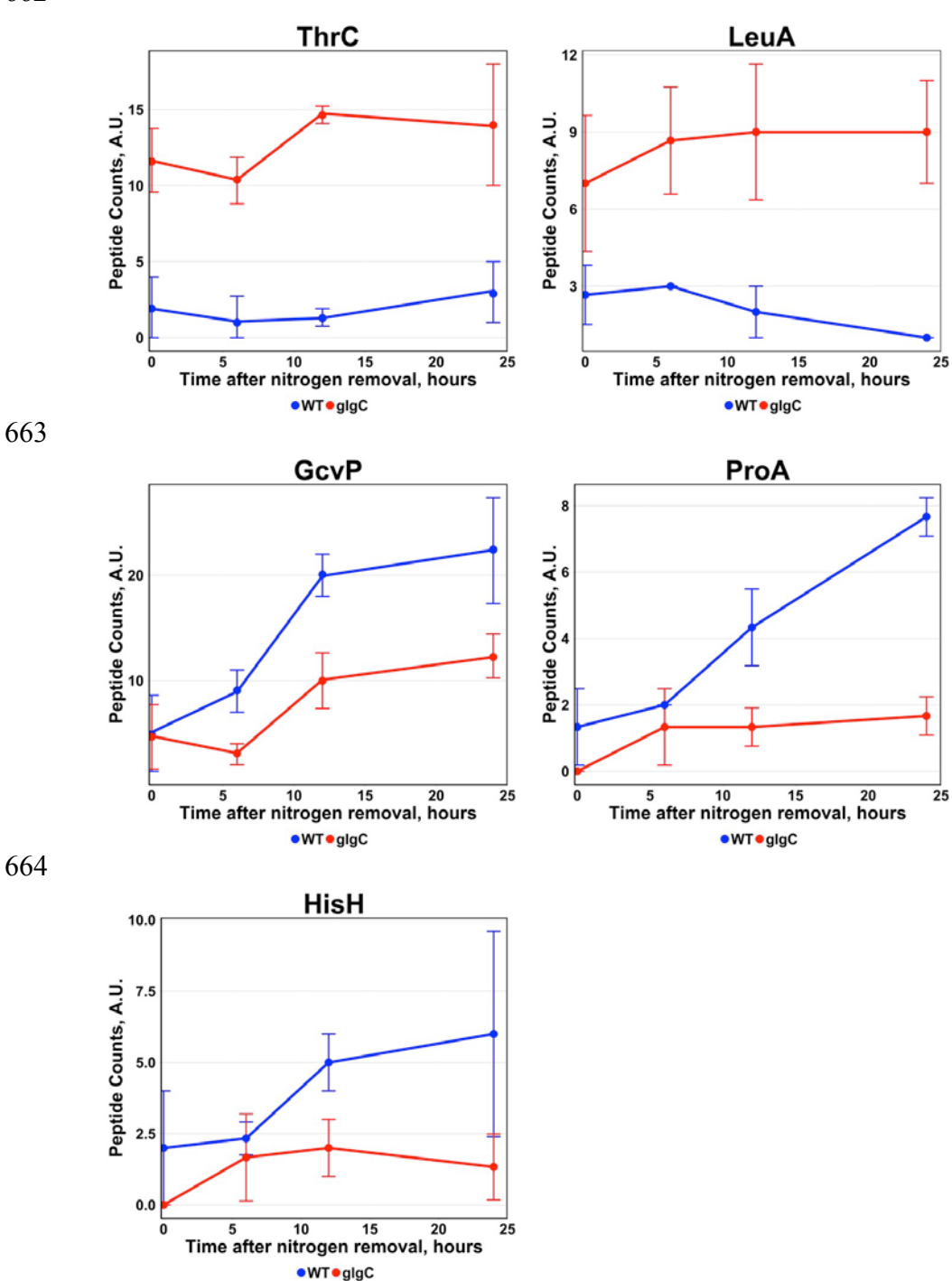


Figure 2: Relative peptide abundances of threonine synthase (ThrC), 2-isopropylmalate synthase (LeuA), glycine dehydrogenase (GcvP), gamma-glutamyl phosphate reductase (ProA), and an amidotransferase (HisH) in WT and  $\Delta glg$ C cells with respect to time after nitrogen removal. Data are presented as arithmetic mean values from 3 independent replicate cultures of each strain. Error bars represent 1 standard deviation from the mean.

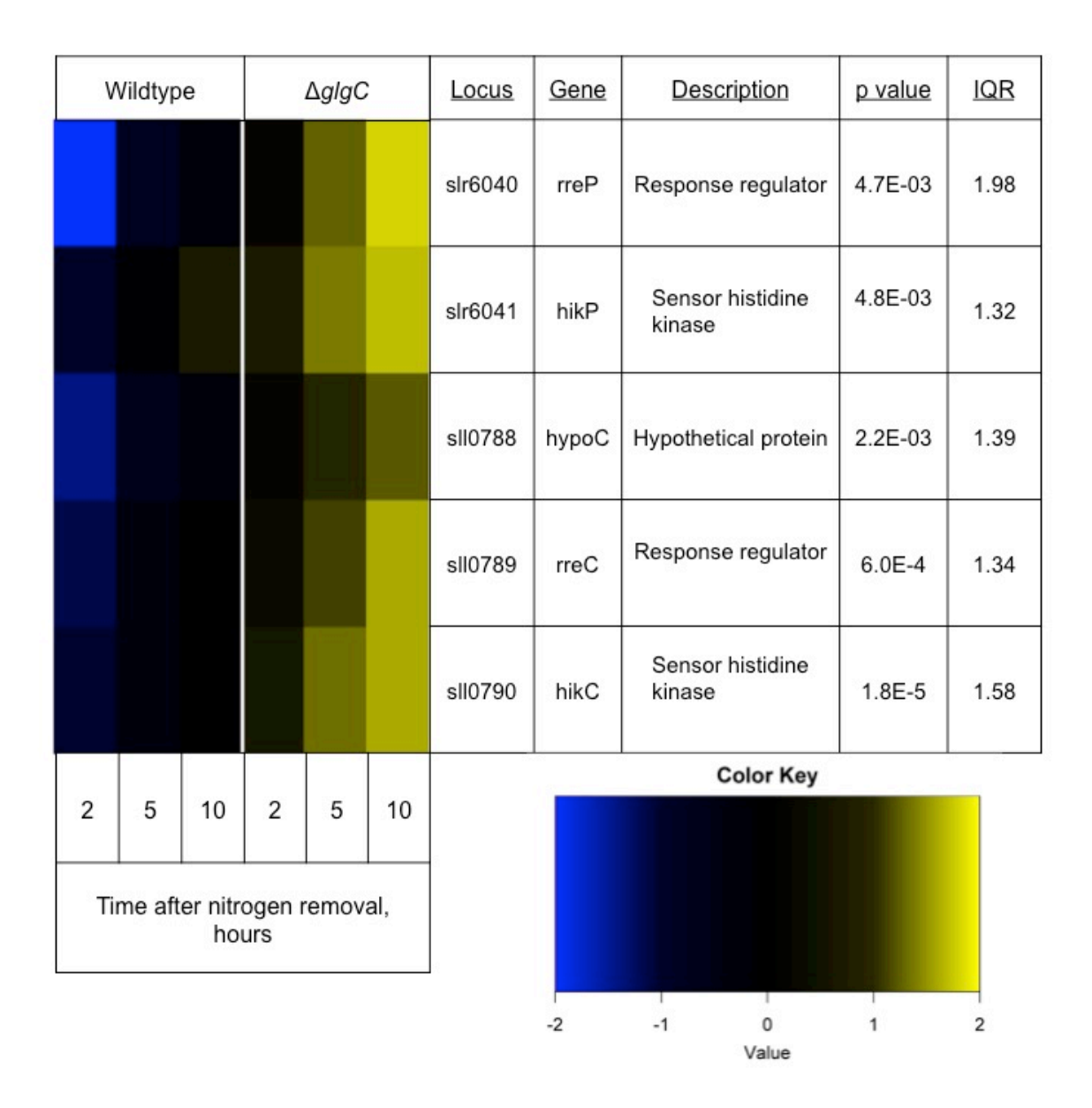
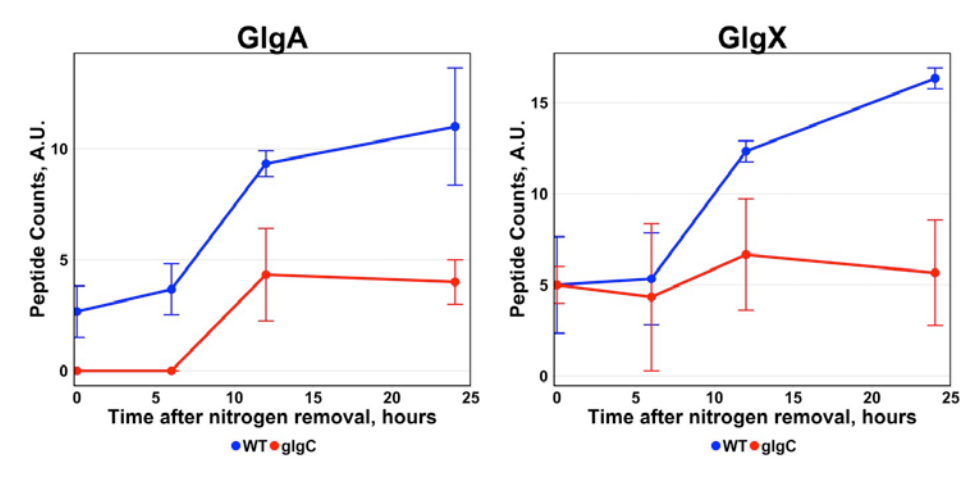


Figure 3: Heat map of transcriptional changes in genes from the *hik*31 operons with respect to time after nitrogen removal from cultures. Color mapped squares represent the geometric means of log<sub>2</sub>(ratios) of transcript abundances at the indicated time relative to transcript abundances before nitrogen removal, n=3.





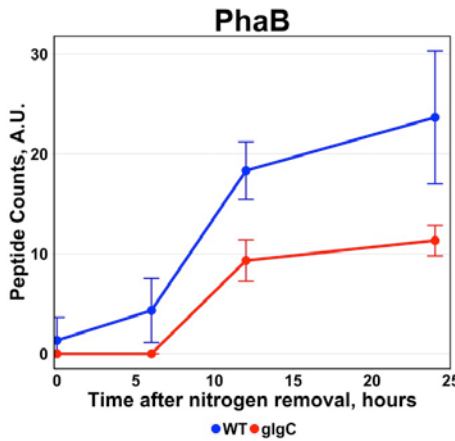


Figure 4: Relative peptide abundances of glycogen synthase (GlgA), glycogen de-branching enzyme (GlgX), and a protein involved in polyhydroxyalkanoate synthesis (PhaB) in WT and  $\Delta glgC$  cells with respect to time after nitrogen removal. Data are presented as arithmetic mean values from 3 independent replicate cultures of each strain. Error bars represent 1 standard deviation from the mean.

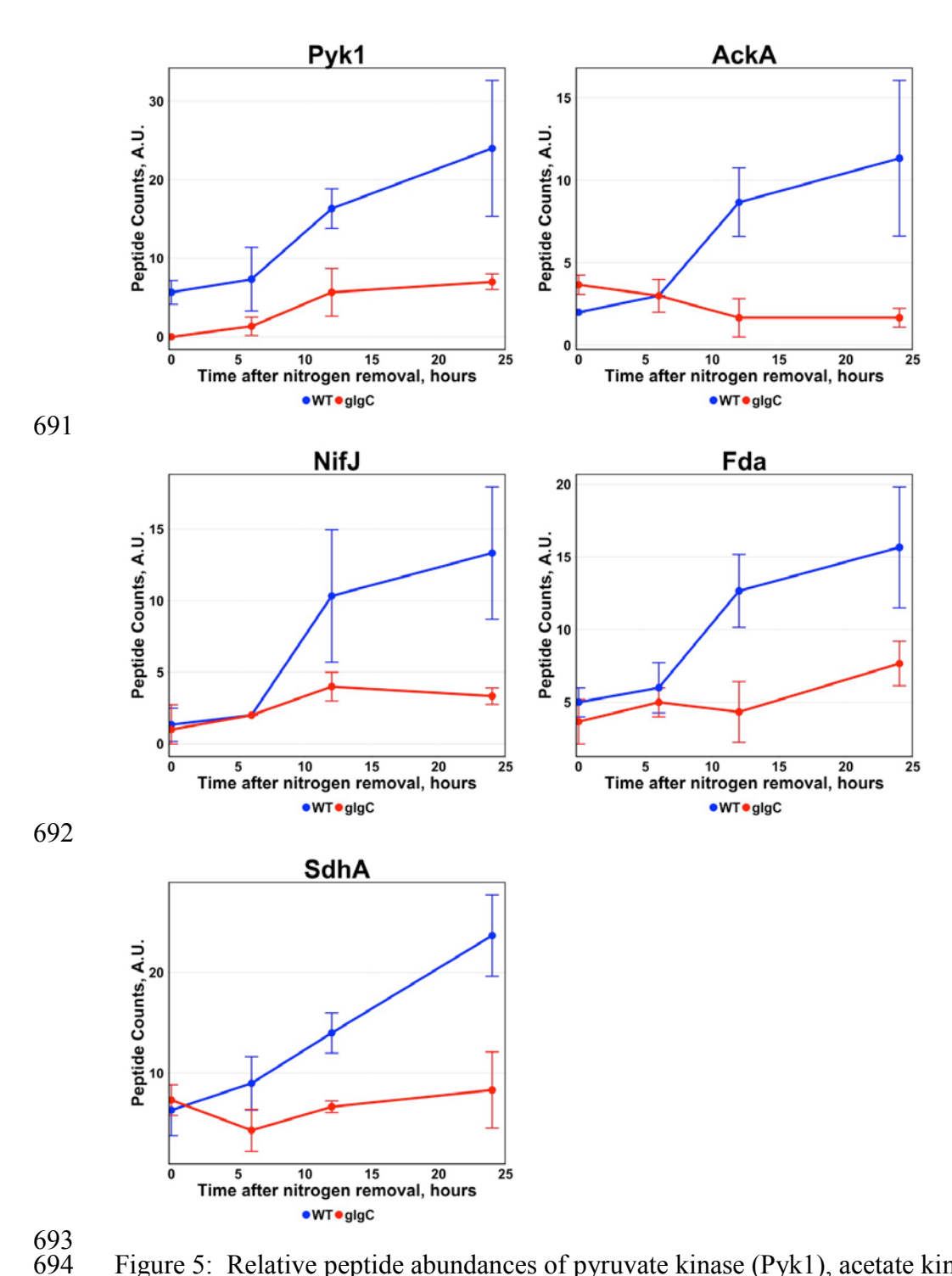


Figure 5: Relative peptide abundances of pyruvate kinase (Pyk1), acetate kinase (AckA), pyruvate flavodoxin oxidoreductase (NifJ), fructose-bisphosphate aldolase (Fda, Class I), and a subunit of succinate dehydrogenase flavoprotein (SdhA) in WT and  $\Delta glg$ C cells with respect to the time after nitrogen removal. Data are presented as arithmetic mean values from 3 independent replicate cultures of each strain. Error bars represent 1 standard deviation from the mean.

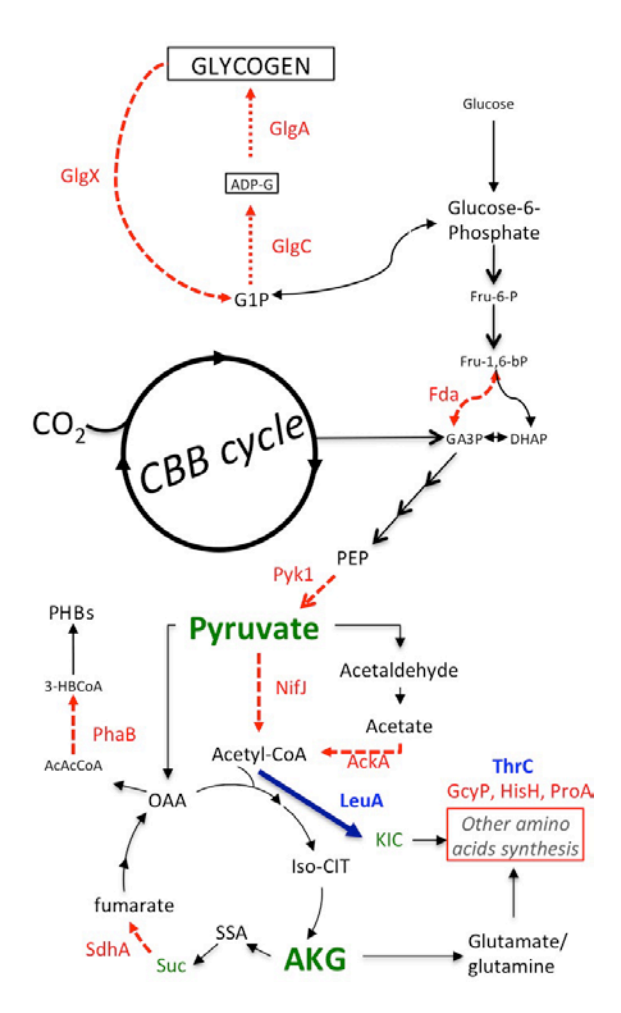


Figure 6: Simplified metabolic scheme for *Synechocystis* WT and  $\Delta glg$ C cells. If higher expression of proteins was observed in  $\Delta glg$ C cells, enzymes arrows and indicators are solid dark blue. If lower expression of proteins was observed in  $\Delta glg$ C cells, enzymes arrows and indicators are dashed lines and red. Metabolites observed extracellularly are in green. Abbreviations: AcAcCoA: acetyl-acetylCoA; ADP-G: ADP glucose; AKG: alphaketoglutarate; DHAP: dihydroxyacetone phosphate; Fru-6-P: fructose 6-phosphate; Fru-1,6-bP: fructose 1,6-bisphosphate; GA3P: glyceraldehyde 3-phosphate; G1P: glucose 1-phosphate; Iso-CIT: isocitrate; KIC: ketoisocaproate; OAA: oxaloacetate; PEP: phosphoenolpyruvate; SSA: succinate semialdehyde; Suc: succinate.

Wildtype		ΔglgC		Locus	<u>Gene</u>	<u>Description</u>	p value	IQR		
						ssl2615	atpH	ATP synthase	9.1E-03	1.63
						sll1321	atp1	ATP synthase	4.3E-02	1.52
						slr0009	rbcL	RuBisCO	1.8E-02	1.89
						slr0011	rbcX	RuBisCO chaperonin	5.6E-03	1.53
						slr0012	rbcS	RuBisCO	9.9E-04	1.80
						sll0247	isiA	High Light & Fe stress protein	3.3E-03	1.39
						ssr2831	psaE	Photosystem I	5.0E-03	1.10
						slr0737	psaD	Photosystem I	7.4E-03	1.04
						sll0819	psaF	Photosystem I	1.3E-02	1.27
						ssr0390	psaK	Photosystem I	1.6E-02	1.51
						slr1835	psaB	Photosystem I	2.2E-02	1.23
			3			sml0008	psaJ	Photosystem I	2.5E-02	1.17
						slr1834	psaA	Photosystem I	5.9E-03	1.67
				2		ssl2542	hliA	High Light stress protein	2.9E-02	1.31
						slr2135	hupE	Hydrogenase	1.1E-02	1.38
						slr1281	nadhJ	NADH dehydrogenase	1.25E-07	1.11
2	5	10	2	5	10	Color Key				
Time after nitrogen removal, hours						١				
							-4	-2 0 2 Value	4	

Figure 7: Heat map of transcriptional changes from genes involved in ATP synthesis, carbon fixation, and photosynthesis with respect to time after nitrogen removal from cultures. Values represent the geometric mean of  $log_2(ratios)$  of transcripts originating from the indicated gene locus for 3 independent replicate cultures of each strain.

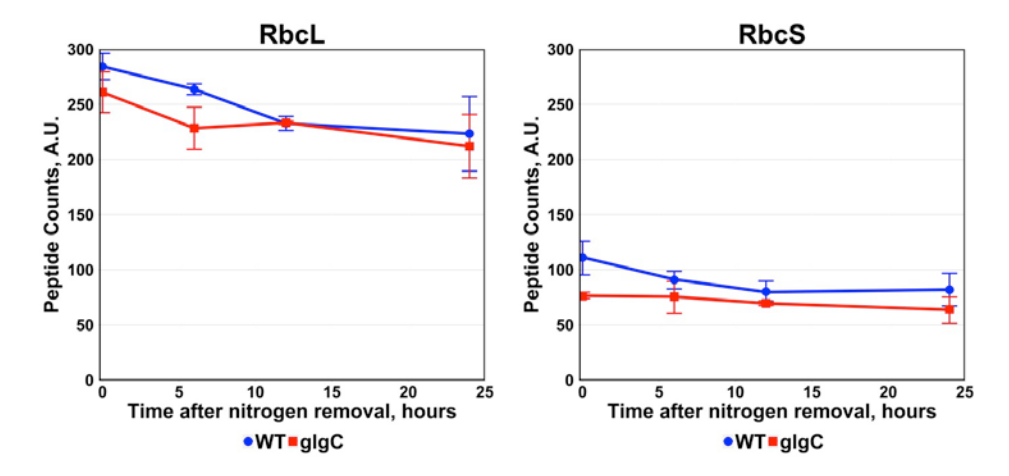


Figure 8: Relative peptide abundances of RuBisCO large (RbcL) and small (RbcS) subunits in WT and  $\Delta glgC$  cells with respect to time after nitrogen removal. Data are presented as arithmetic mean values from 3 independent replicate cultures of each strain. Error bars represent 1 standard deviation from the mean.

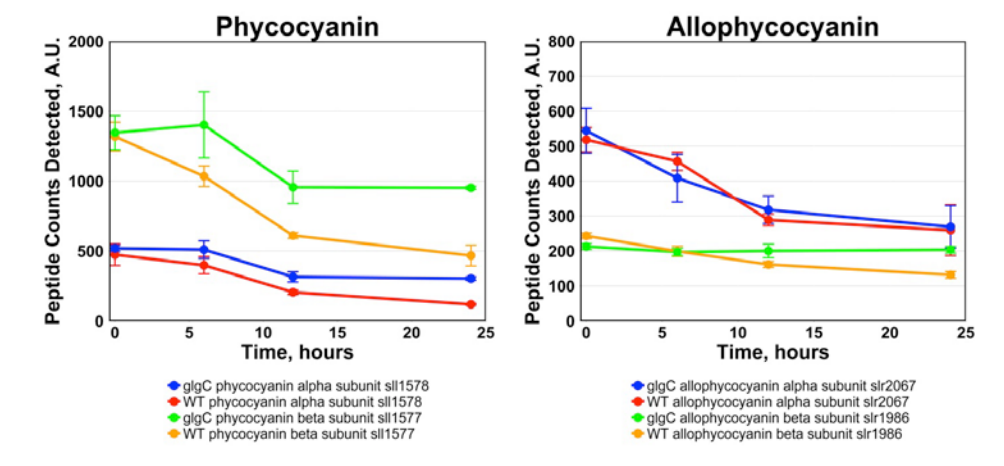


Figure 9: Relative peptide abundances of phycocyanin and allophycocyanin alpha and beta subunits in WT and  $\Delta g/g$ C cells with respect to time after nitrogen removal. Data are presented as arithmetic mean values from 3 independent replicate cultures of each strain. Error bars represent 1 standard deviation from the mean.